Pang et al. Radiation Oncology (2025) 20:64
https://doi.org/10.1186/s13014-025-02648-1

Radiation Oncology

RESEARCH

Open Access

The investigation of opening modes of head and neck thermoplastic mask for radiotherapy based on finite element analysis

Guobao Pang[1], Ying Lu[1,2], Yannan Xu[1], Qiaoyu Meng[3*] and Jianbo Song[1*]

Abstract
Radiotherapy is a crucial treatment modality for head and neck tumors. Precise patient positioning is vital for ensuring the reproducibility and accuracy of the treatment. Clinically, thermoplastic head and neck masks are used for positioning, and patients often require openings in these masks. However, the relationship between opening locations and the fixation effectiveness of the masks has not been thoroughly studied. This study reconstructs a patient's imaging data to create finite element models with 10 different opening patterns. By assigning various thicknesses and material properties to the fixation masks, we analyzed the displacement distribution of different opening models under diverse loading conditions. The results indicate that the opening location significantly impacts fixation effectiveness under different loading conditions. In particular, the opening in the forehead area has the most significant impact on the fixation effect of the mask near the region of interest (ROI). Therefore, in clinical practice, the design of openings in the forehead area should be carefully considered. This study provides valuable insights into the fixation effectiveness of thermoplastic masks and serves as a reference for future personalized positioning treatments.

Keywords Radiotherapy, Head and neck tumors, Head and neck thermoplastic mask, Fixation effectiveness, Finite element analysis

*Correspondence:
Qiaoyu Meng
m_qiaoyu@163.com
Jianbo Song
jianbo2611@sxmu.edu.cn
[1]Cancer Center, Tongji Shanxi Hospital, Shanxi Bethune Hospital, Shanxi Academy of Medical Sciences, Third Hospital of Shanxi Medical University, Taiyuan, China
[2]Shanxi Provincial Key Laboratory for Translational Nuclear Medicine and Precision Protection, Taiyuan, China
[3]Institute of Advanced Structure Technology, Beijing Institute of Technology, Beijing, China

Introduction

Head and neck cancers encompass malignant tumors in regions such as the oral cavity, larynx, and pharynx, accounting for 6–8% of global cancer cases [1], with approximately 710,000 new cases reported in 2018, primarily consisting of oral cancer, laryngeal cancer, and nasopharyngeal carcinoma [2–4]. Radiotherapy has emerged as a cornerstone modality for X-ray-sensitive tumors like nasopharyngeal carcinoma, tonsil cancer, and laryngeal cancer, due to its precision and organ preservation benefits. It achieves local control by disrupting the DNA of tumor cells with high-energy radiation, while minimizing surgical damage to functions such as swallowing and speech [5–9]. Its indications span curative treatment, postoperative adjuvant therapy, and multimodal combination therapy, significantly reducing the risk of recurrence and optimizing functional outcomes [10–12].

Therefore, the role of radiotherapy in the treatment of head and neck tumors is significant and worthy of our enough attention. It can effectively control disease progression while enhancing patients' quality of life and prolonging survival duration. However, radiotherapy may also bring some side effects, such as vocal cord edema, dry mouth, change of taste, nausea, etc [13, 14]. Therefore, there are high demands for the precision of radiotherapy for head and neck tumors.

Image-guided techniques are often used in radiotherapy to correct positional errors [15, 16]. These techniques include kilovoltage cone-beam CT (CBCT), megavoltage cone-beam CT (MVCT) etc., which can correct errors in X, Y, Z axis. Nevertheless, most medical linear accelerators in developing countries remain incapable of compensating for 3D rotational deviations (pitch, roll, and yaw) frequently observed in head and neck radiotherapy patients. While 6D couch systems are increasingly incorporated into standard clinical protocols, their corrective capacity remains constrained for head and neck malignancies due to the inherent deformative characteristics of planning target volumes (PTVs). Hirotaki et al. found that the anatomy of the head and neck undergoes significant changes during the course of radiotherapy, with positional errors in various directions varying with the number of treatment days [17]. For instance, in the anterior-posterior direction, the positional errors of structures such as vertebrae are large and increase over time; similar trends are also observed in the pitch direction for some structures. Despite the use of Six Degrees of Freedom (6DOF) automatic image registration methods with different regions of interest (ROIs), complete resolution of the issues arising from anatomical changes and positioning errors remains elusive in intensity-modulated proton therapy. The effectiveness of reducing the dose to organs at risk (OARs) is also suboptimal, highlighting the limitations of relying solely on 6DOF alignment for complete positional correction [17]. Therefor, this study emphasizes the critical role of immobilization efficacy in achieving optimal dose conformity.

Most of the auxiliary fixation devices used in radiotherapy for head and neck tumors nowadays are head and neck immobilization masks with mesh openings, which are made of a special thermoplastic material with a specific softening point temperature [18]. During the process, the thermoplastic film is heated to a softening point and then applied to the patient's head and neck area. The thermoplastic film is attached to the treatment bed by means of surrounding clasps and immobilization is completed when the material has cooled and hardened.

However, in clinical practice, it is often necessary to make openings in different parts of the head and neck immobilization mask based on the patient's specific conditions. For example, during the treatment process, some patients may experience symptoms of claustrophobia and need to have openings made in specific locations in the fixation membrane to alleviate the symptoms [19, 20]. Elsner et al. found that up to 49% of head and neck cancer (HNC) patients experience distress and anxiety due to immobilization devices during the course of radiotherapy, particularly before treatment commences [21]. In addition, some patients require special procedures such as nasal feeding, tracheal intubation, or the use of an oral mouthpiece, which also requires perforation at specific sites to ensure therapeutic efficacy and safety. Some patients may have wounds on the head and neck, which may also need to be pierced to avoid infection.

Open-Face Masks (OFMs) significantly enhance patient comfort by exposing specific facial areas, such as the forehead, eyes, and nose, while maintaining immobilization accuracy and repeatability. Lastrucci et al. reviewed the heterogeneous research on the application of OFMs in head and neck and brain cancer radiotherapy, finding diverse types and usage patterns. However, most studies demonstrated that OFMs combined with Surface Guided Radiation Therapy (SGRT) offer significant advantages in patient comfort and positioning accuracy [22]. Keane et al. conducted a randomized controlled trial showing that open-face masks markedly improve patient comfort, with the majority of patients preferring them over traditional masks [23]. Chen X et al. innovatively developed an open-face mask compatible with SGRT, which, when used with a custom headrest and bite block for brain stereotactic radiotherapy, exhibited superior positioning precision and stability compared to the traditional closed-face mask combined with the Fraxion positioning system [24].

However, there is a lack of intuitive and quantitative evaluation research on the relationship between the location, shape, and other parameters of the openings and the effectiveness of the head and neck immobilization mask fixation. Fisher et al. performed a pre-clinical evaluation of a fixation system for patients receiving radiotherapy for head and neck tumors [25]. They used CT images of the patient's face to extract facial features and created a 4 mm thick mask model. The CT scans were re-scanned with the mask attached, and analyzed using Hausdorff distance. The study showed a median "worst case" tolerance of about 4 mm for more than 80% of slices, suggesting that the resulting mask is capable of achieving a fixed level similar to the current system. However, the study only considered the construction of the facial model and did not connect it to the treatment Table [25]. Chen et al. proposed an automatic framework for constructing and manufacturing a fixation mask for head and neck radiotherapy [26]. Loja et al. extracted geometric information of the standard human head using both CT and 3D scanners, and designed three types of radiotherapy head fixation masks with different openings. Finite element methods were used to evaluate the stress and strain of the various opening masks under typical loads [27]. However, the models they used were standard models of human heads, and did not consider the research process for patients with large individual differences in clinical practice. Additionally, the opening structures required by different patients may not be the same, thus further analysis of fixation effectiveness under different opening conditions is still needed to be explored.

In this study, a personalized head and neck fixation membrane model was established for a patient undergoing radiotherapy for head and neck tumor. Ten opening conditions were designed, and finite element analysis was used to analyze the deformation size and location of different opening models under various loads. The results of this study can help physicians better understand the effect of fixed membrane opening on the fixation effect in radiotherapy of head and neck tumors, and guide physicians to select the appropriate location and size of the opening to improve the fixation effect, radiotherapy efficacy and patient treatment experience. Additionally, this study provides a new research idea for issues related to opening structures of fixation masks.

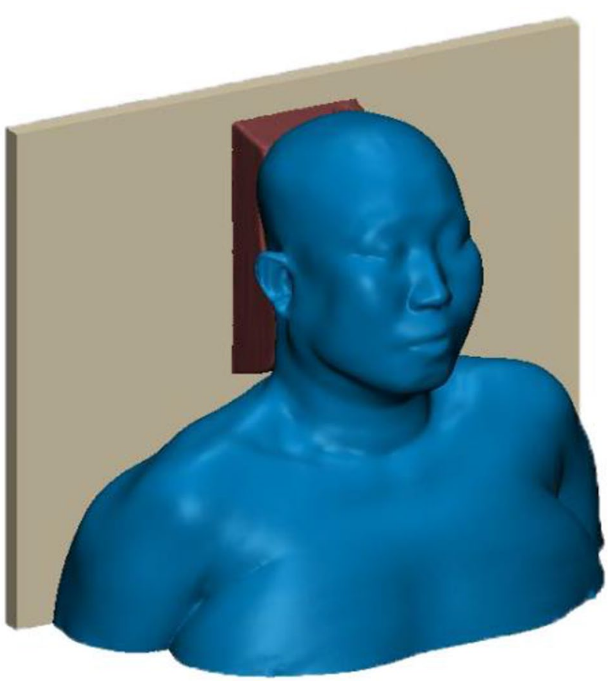

Fig. 1 Head and neck geometry mode

Materials and methods

Data acquisition

In this study, we selected head and neck CT localization images of a patient with sinus cancer diagnosed by the Cancer Center of Shanxi Bethune Hospital. The patient was a 55-year-old female who was admitted on January 29th, 2023. We performed a localization CT scan of the patient using the Philips Brilliance Bigbore and planned to administer TOMO radiotherapy. This study was approved by the Ethics Committee of Shanxi Bethune Hospital (YXLL-2022-127), and strictly complied with the relevant regulations of medical ethics and the requirements of patients' informed consent.

Head and neck thermoplastic mask model

The scanning layer thickness of radiotherapy localization CT images for head and neck tumor patients was 3 mm, with 165 slices in total. The images were reconstructed using the CT reconstruction software, and the thickness of the reconstructed slice was 1 mm, with a total of 423 slices. Subsequently, the images were imported into MIM Software Inc, and the body, headrest, and bed were delineated and moderately smoothed to obtain their respective structures and exported as STL files. The above geometric models were smoothed by Laplacian using Materialise 3-matic software to obtain higher quality and smoother geometric models, as shown in the Fig. 1.

By cropping the geometric model of the head and neck, we neatly remove the part of the head behind the ear in the sagittal plane. Then, we stretch along the incision in the sagittal plane towards the back of the model until it reaches the bed, obtaining the geometric model of the head and neck fixation mask. Ten common types of openings required for head and neck fixation membranes during radiotherapy were selected, they are mouth, nostrils and forehead (A), mouth, nostrils and eyes (B), mouth, nostrils, eyes and forehead (C), mouth and nose (D), mouth, nostrils and chin (E), mouth, nostrils and throat (F), mouth, nostrils and shoulders (G), mouth, nostrils and collarbone (H), mouth and nostrils (I), full face (J), as shown in the Fig. 2.

Masks' material properties

A total of five different materials of unperforated thermoplastic films were selected, two from Guangzhou Klarity Medical & Equipment were labeled as M_1, M_2, and three from Guangzhou Renfu Medical & Equipment were labeled as M_3, M_4, and M_5, respectively.

The thermoplastic film is regarded as a linear elastic material, and the modulus of elasticity and Poisson's ratio need to be set in the simulation software. Five sets of standard tensile test samples are prepared for each material according to the national standard GB/T 1040.2–2022, and the shape of the specimens is shown in Fig. 3.

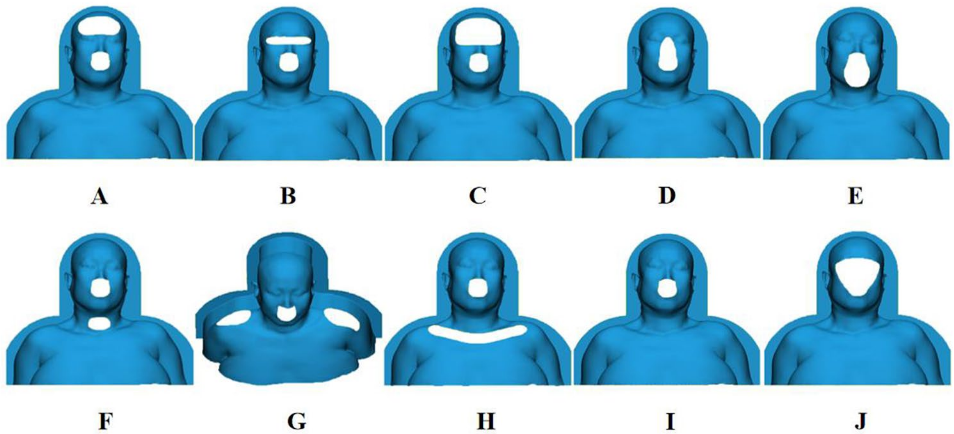

Fig. 2 Ten kinds of models

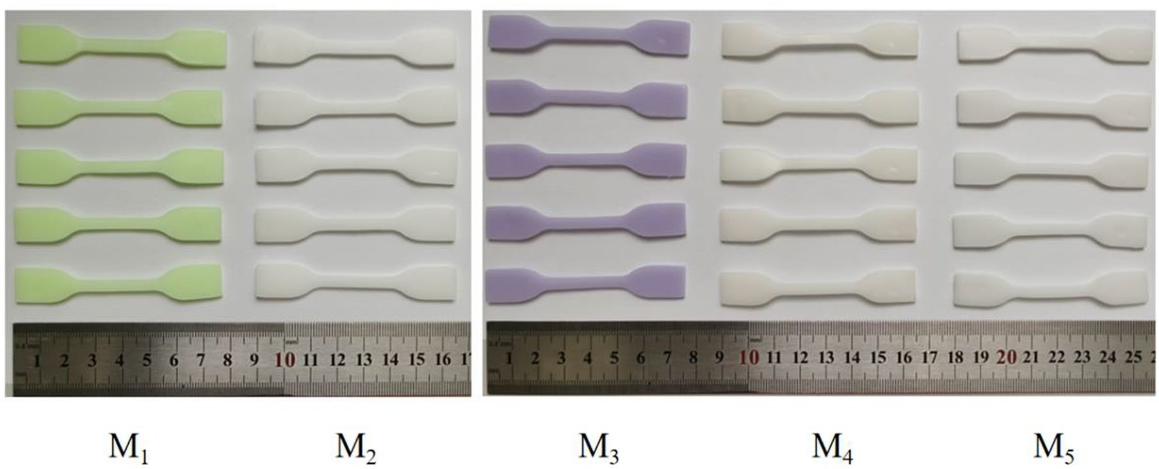

Fig. 3 Tensile test samples

Quasi-static tensile tests were performed on an Instron 5544 universal testing machine with the stretching rate set at 0.5 mm/min. Since the thermoplastic film has large deformations in the scale-spaced section during stretching, the measured engineering stress σ_e and engineering strain ε_e are not the true stress σ_t and true strain ε_t of the material. These values must be corrected using the following equation:

$$\begin{aligned}\sigma_t &= \frac{F}{A_t} = \frac{\sigma_e \times A_0}{A_t} = \frac{\sigma_e \times \frac{V}{L_0}}{\frac{V}{L_t}} \\ &= \sigma_e \times \frac{L_t}{L_0} = \sigma_e \times \frac{(L_0 + \Delta L)}{L_0} \\ &= \sigma_e \times (1 + \epsilon_e)\end{aligned} \quad (1)$$

$$\begin{aligned}\epsilon_t &= \int_{L_0}^{L_t} \frac{dL}{L} = dlnL \,\Big|_{L_0}^{L_t} = lnL_t - lnL_0 \\ &= ln\frac{L_t}{L_0} = ln\frac{L_0 + \Delta L}{L_0} = ln(1 + \epsilon_e)\end{aligned} \quad (2)$$

where F is the tensile force, A_0 and A_t are the initial and true cross-sectional areas of the spar section, L_t and L_0 are the length of the true interval and the initial interval, L is the specimen length, and V is the volume of the spar section. During yielding and subsequent plastic flow, the volume change due to material flow is negligible because the effect of increased length is offset by the decrease in cross-sectional area. Before necking, the strain remains the same along the entire length of the specimen. The elastic modulus of the material was calculated according to the real stress-strain curve fitting after conversion, and Poisson's ratio was calculated by measuring the size of the standard distance segment of the thermoplastic film in the linear elastic stage, and the average value of the five groups of data was obtained.

Finite element simulation

The thicknesses of the head, neck and shoulder fixation membranes commonly used at present are 1.6 mm, 2.0 mm, 2.4 mm and 3.0 mm. In this paper, 200 models are modeled by setting the above four thicknesses for each type of opening and assigning the above tested five material properties to them respectively. The stresses and displacements occurring in various models of the human head under two working conditions, left rotation and flexion, were simulated in the finite element commercial software Abaqus 2020. Abaqus is a powerful engineering simulation software based on finite element method. It can solve problems ranging from simple linear problems to very complex nonlinear simulations. Because of its powerful simulation function, it is used by engineering researchers all over the world, and has become the most widely used finite element analysis software in simulation research. Abaqus provides users with a wide range of functions and is very easy to use. Therefore, this paper chooses the 2020 version of Abaqus software as the simulation tool. The analysis process of Abaqus usually has three steps: pre-processing, simulation calculation, and post-processing. In the pre-treatment process, the geometric model should be established first. Secondly, the model is endowed with material properties; Loads and boundary conditions are then applied to the model. The calculation process usually runs in the background. Save the output data as stl format file. The post-processing process is carried out interactively in the graphical environment through the visualization module. Display binary results as image results or graphs. A total of 400 simulations were calculated. The size of the applied load comes from a study by Almosnino [28], who used sensors to measure the forces generated by athletes' heads when they turned left and when they bent, and obtained forces of 157.2 N and 149.7 N, respectively.

The force values of 157.2 N and 149.7 N applied to the mask were based on the research data of Almonsino et al., rather than the results of mechanical experiments conducted on patients by us. The 55-year-old patient did not participate in the head-turning and head-lifting experiments under the 10 types of opening models, and it is difficult for the human body to precisely control the magnitude of the force applied during head-turning and head-lifting. We used the CT image of one patient to create a 3D model of the mask by reconstructing the surface of the body, and then applied the head-turning and head-lifting forces in the finite element simulation software according to the force values obtained in the study by Almonsino et al. During the simulation process, we were able to precisely control the magnitude and application range of the head-turning and head-lifting forces under the 10 types of opening models, ensuring their complete consistency, thereby making the opening type the only variable.

The boundary condition is a kind of restrictive condition that constrains the finite element model. In this study, the boundary condition is a restrictive condition that constrains a certain part of the model, thus keeping the model fixed. Boundary conditions are also crucial to ensure the accuracy and reliability of the analysis results. In finite element analysis, the determination of boundary conditions is an important part of the establishment of finite element model, and reasonable determination of the boundary conditions of finite element model is the basic requirement for successful finite element analysis of structures. In the clinic, the thermoplastic film needs to be fixed and tightly attached to the treatment bed. Therefore, the fixed part of the thermoplastic film and the treatment bed sets the region for the boundary conditions. The boundary conditions and load diagram are shown in Fig. 4. The red line in Fig. 4 (a) is the area where the boundary conditions are applied. In the finite element software, the displacement and angle range of the red line region are all set to 0. Through the calculation in the finite element software, we can obtain the deformation of different open mask models under the two loads. In the finite element calculation results, we can see the specific size of the deformation at any point on the mask. For the loading of 10 kinds of masks and related test content, all work is done on the computer. Specifically, we contoured the body of the patient's CT image and reconstructed the part in three dimensions and modeled it. All mask types and the load application process were carried out in a computer, not with a real mask, and were not tested on the patient body.

Results and discussion

The elastic modulus of the mask

The displacement-force curve of the tensile test is shown in the Fig. 5. The elastic modulus of the five materials is shown in Table 1. The results reported by Loja et al. [26] are close to those calculated in this paper.

The effect of thickness on the deformation of the mask

When the material modulus was set to M_1, the maximum deformation of the head and neck shoulder fixation mask with 10 types of openings under two loads is shown in the following Fig. 6. After calculating, the results of other elastic modulus parameters were similar.

The figure shows the maximum deformation (unit: cm) under different loading conditions (roll and up) for four different mask thicknesses (1.6 mm, 2.0 mm, 2.4 mm, and 3.0 mm). With the increase of mask thickness, the maximum deformation gradually decreases under all types of openings. At the thickness of 1.6 mm, the deformation ranges from 2.15 cm to 3.95 cm; at the thickness

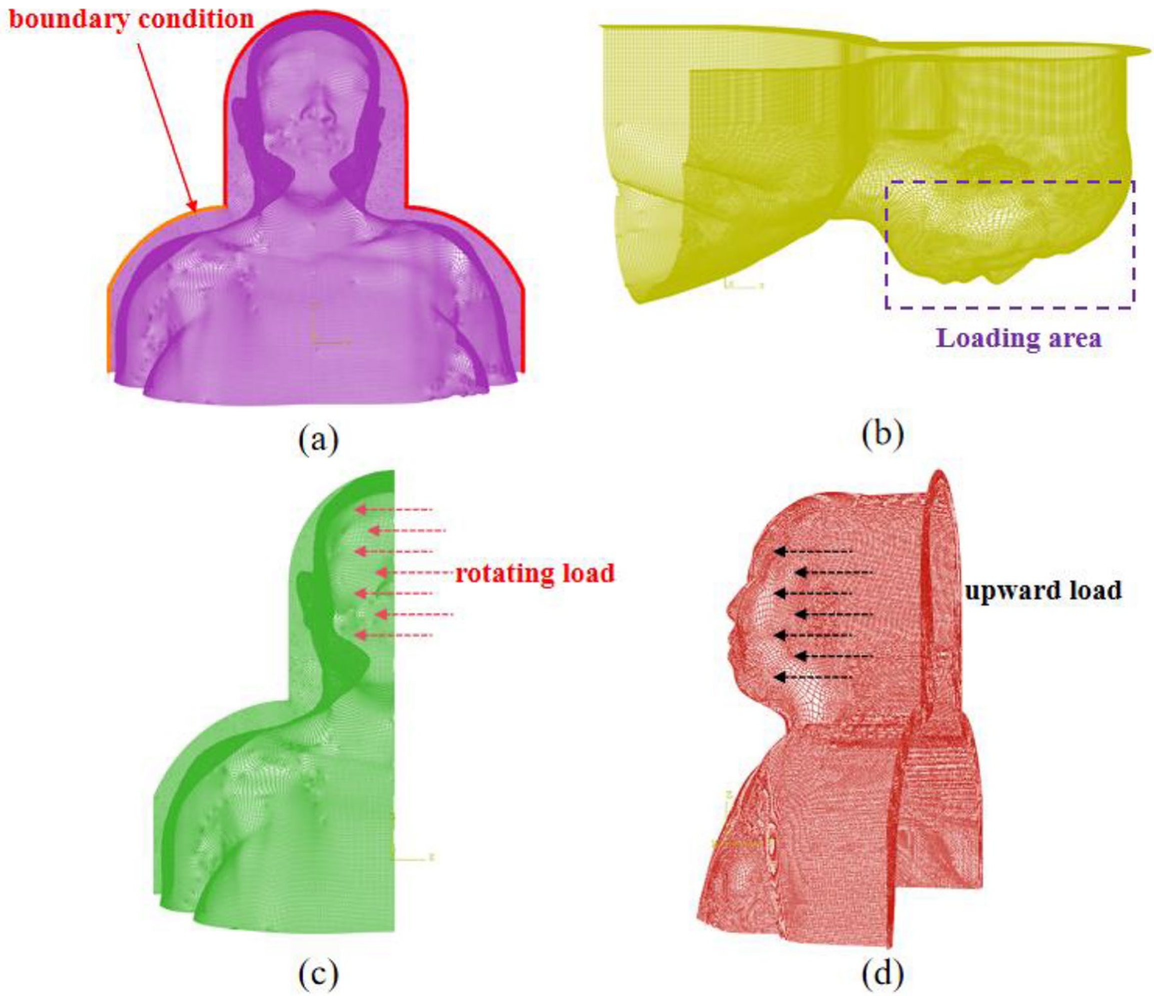

Fig. 4 The diagram of boundary condition and loading. (**a**) boundary condition, (**b**) loading area, (**c**) rotating load, (**d**) upward load

of 2.0 mm, the range of deformation narrows to 1.21 cm to 2.08 cm; at the thickness of 2.4 mm, the deformation further reduces to 0.56 cm to 1.22 cm; finally, at the thickness of 3.0 mm, the maximum deformation is the smallest, ranging from 0.31 cm to 0.69 cm.

It can be seen from the figure that under the rotation and upward load conditions, the maximum deformation of the head and neck shoulder fixation mask with 10 types of openings is the greatest when the thickness is 1.6 mm, and decreases successively when the thickness is 2.0 mm, 2.4 mm, and 3.0 mm. In general, the maximum deformation decreases with increasing mask thickness.

This trend indicates that increasing thickness can effectively reduce the deformation of the fixation mask, suggesting that choosing a thicker fixation mask can help reduce positioning errors. Currently, the most commonly used thickness for head and neck shoulder fixation films in clinical radiotherapy is 2.4 mm. Whenever possible, masks with a thickness of 3.0 mm should be used to minimize positioning errors. It is worth noting that although increasing the thickness of the mask can significantly enhance the immobilization effect, it may also exacerbate claustrophobia in patients, particularly among sensitive patient groups. Thicker masks can restrict the perception of breathing and enhance the sensation of physical pressure, potentially inducing anxiety or panic reactions, which may lead to treatment interruptions or positional shifts. Therefore, in clinical practice, it is necessary to balance the immobilization requirements with the psychological tolerance of patients. In the future, we will further quantify the correlation between mask thickness and claustrophobia scores and explore thickness thresholds or personalized designs to better reconcile the trade-off between immobilization effectiveness and patient comfort. Additionally, thicker masks may also have a certain impact on patient skin dose. The yield of low-energy scattered photons increases in thicker masks, potentially raising the absorbed dose to the epidermis, especially when using low-energy beams (such as kilovoltage X-rays). During radiotherapy, the mask is in close

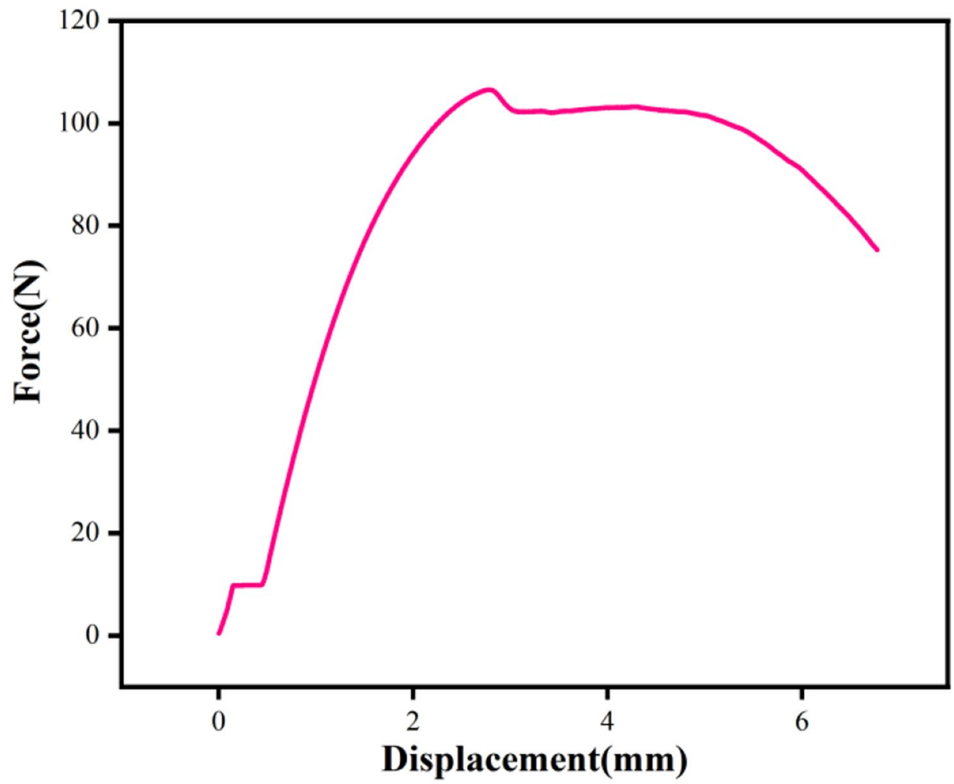

Fig. 5 Sample load-displacement curve

Table 1 Material properties

Material type	M_1	M_2	M_3	M_4	M_5
Modulus(GPa)	3.83	2.68	3.57	2.45	3.43

contact with the skin. Thicker masks may enhance the emission of secondary electrons, leading to an increase in surface dose. Moreover, thicker masks may alter the build-up effect of the primary beam, which needs to be corrected in the treatment planning system using Monte Carlo algorithm or measured data. In Intensity-Modulated Radiation Therapy (IMRT), the dose distribution

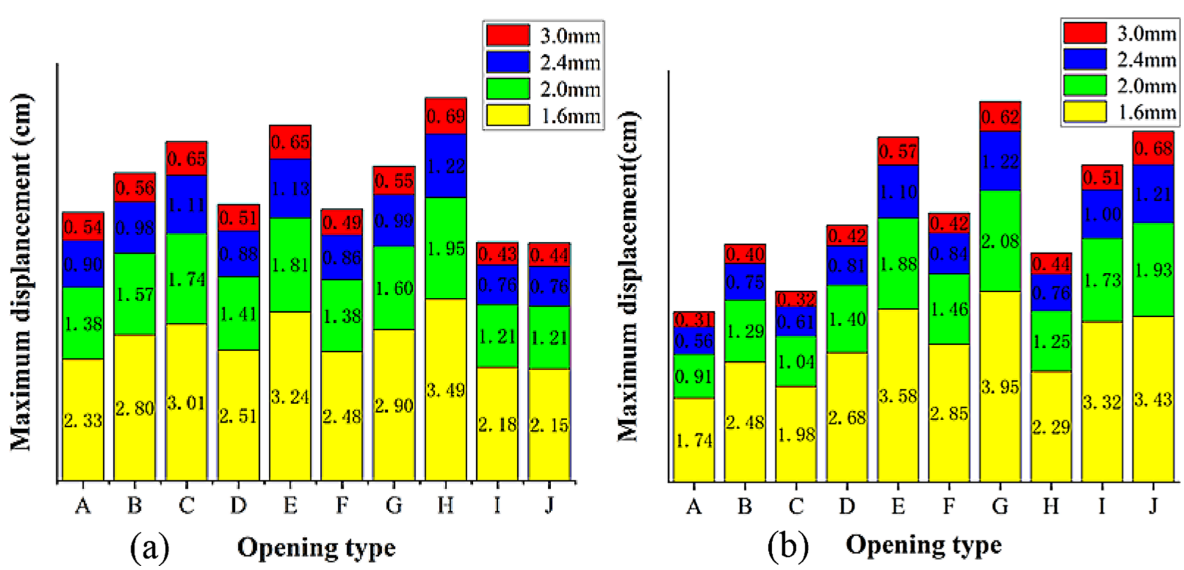

Fig. 6 (**a**) The maximum displacement of the mask under rotating load when the elastic modulus of the material is M_1. (**b**) The maximum displacement of the mask under upward loading when the elastic modulus of the material is M_1

should be re-validated to ensure that the skin dose does not exceed the tolerance limits.

The effect of material properties on mask deformation

The elastic modulus of the five thermoplastic membrane materials is shown in Table 1. When the material thickness is set at 2.4 mm, the maximum deformation of the head and neck shoulder fixation masks with ten types of openings under two types of loads varies with the elastic modulus of the materials, as illustrated in Fig. 7. Similar calculations were conducted for the other materials as well. The results show that regardless of the elastic modulus of the material, the trend in the maximum deformation curves for the fixation masks remains consistent with the trend observed in Fig. 7.

The figure shows that under both rotational and upward loads, the maximum deformation of the 10 types of head and neck shoulder fixation films decreases linearly with increasing material elastic modulus. This indicates that a higher elastic modulus of the material results in smaller positioning errors when using the of head and neck shoulder fixation films.

In practice, the head and neck shoulder fixation masks are composed of various materials such as PMMA, low-density polyethylene, and paraffin, making them not truly linearly elastic materials. In this study, the fixation films were simplified as linearly elastic materials for the following reasons: First, the fixation film materials exhibit viscoelastic or elastoplastic properties, and the constitutive relationships for these properties are complex, making it difficult to determine the parameters of the constitutive models. Second, the loading conditions in the simulation involve relatively small forces and deformations. In the small deformation regime, the stress-strain relationship of the fixation films can be approximated as linear. Therefore, it is reasonable to treat the fixation films as linearly elastic in the simulation.

Additionally, variations in the composition of fixation films from different manufacturers lead to differences in elastic modulus results. The five materials selected for elastic performance measurement in this study may not be fully representative and should be considered as references.

The effect of opening position on mask deformation

The strains occurring in the head and neck shoulder fixation masks with 10 different opening types, commonly utilized in clinical settings with a material elasticity modulus of M_1 and a thickness of 2.4 mm under rotational loading, are presented in Fig. 8.

From the displacement diagram, it can be observed that the maximum displacement occurs near the nose for both opening types A (mouth, nostrils, and forehead) and C (mouth, nostrils, eyes and forehead), with the maximum displacements being 0.9 cm and 1.1 cm, respectively. For the remaining eight opening methods, the maximum displacements all occur at the bottom edge of the head and neck immobilization mask. The range of maximum displacement is from 0.75 cm to 1.2 cm.

In clinical practice, we focus more on the displacement of the head and neck immobilization masks. Smaller displacements indicate better fixation performance. Research has demonstrated that precise positioning is critical for ensuring accurate dose delivery, with improved fixation directly correlating to enhanced dosing accuracy [29]. For the A and C opening patterns, the opening area on the forehead is relatively large. Moreover, the force is applied to the side of the face, which

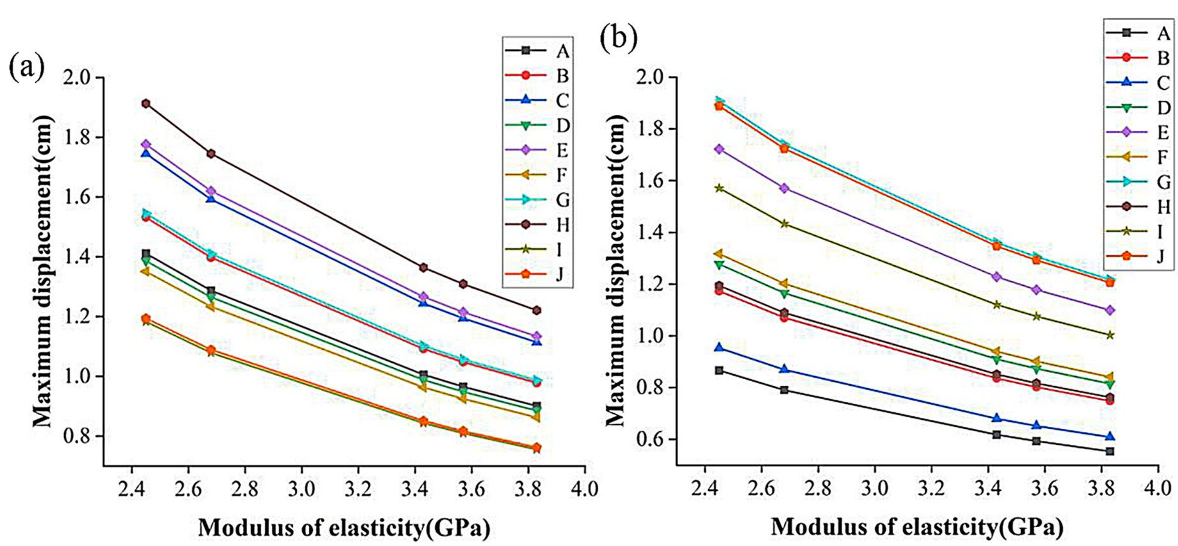

Fig. 7 (**a**) The maximum displacement of the mask under rotating load when the thickness is 2.4 mm. (**b**) The maximum displacement of the mask under upward loading when the thickness is 2.4 mm

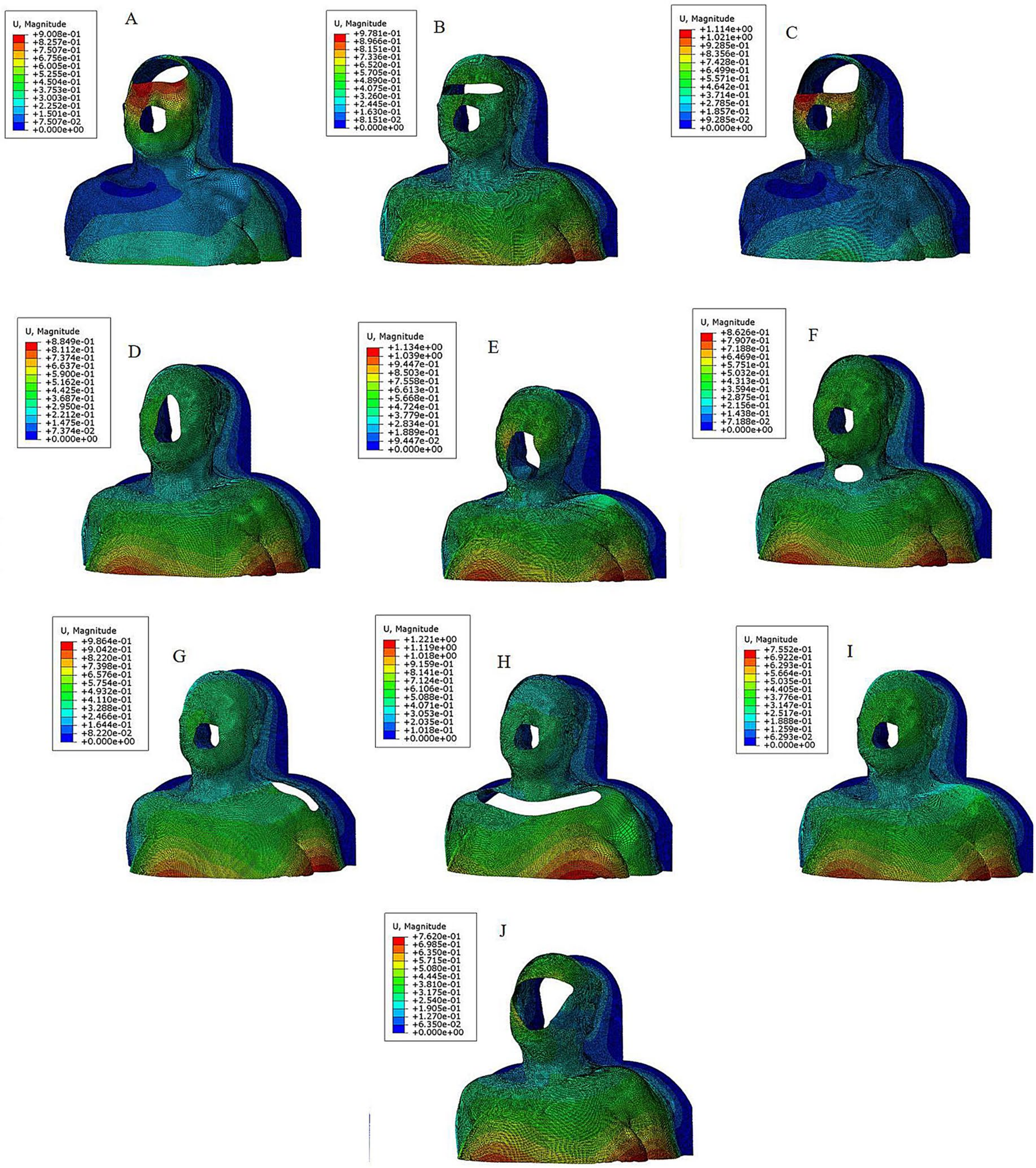

Fig. 8 The displacements of head and neck shoulder fixation masks with 10 different opening types (**A**: mouth, nostrils, and forehead; **B**: mouth, nostrils and eyes; **C**: mouth, nostrils, eyes, and forehead; **D**: mouth and nose; **E**: mouth, nostrils and chin; **F**: mouth, nostrils, and throat; **G**: mouth, nostrils, and shoulders; **H**: mouth, nostrils, and collarbone; **I**: mouth and nostrils; **J**: full face) under rotational loading

can lead to an overall decrease in the fixation effect on the face. Although the J model also has a large opening area, the reduced force application on the face results in smaller overall facial displacement. As for the other eight models besides A and C, there is a larger displacement at the edge of the chest. This is due to the poor constraint at the edge of the chest area of the model.

Under upward loading conditions, the strains of the 10 types of head and neck fixation masks are shown in Fig. 9.

From the displacement diagram, it can be observed that the range of maximum displacement is from 0.55 cm to 1.22 cm. The models with poorer fixation performance are A, B, H, and J. For model A, the maximum displacement occurs near the nose, with a maximum value of 0.55 cm. For model B, the maximum displacement is also

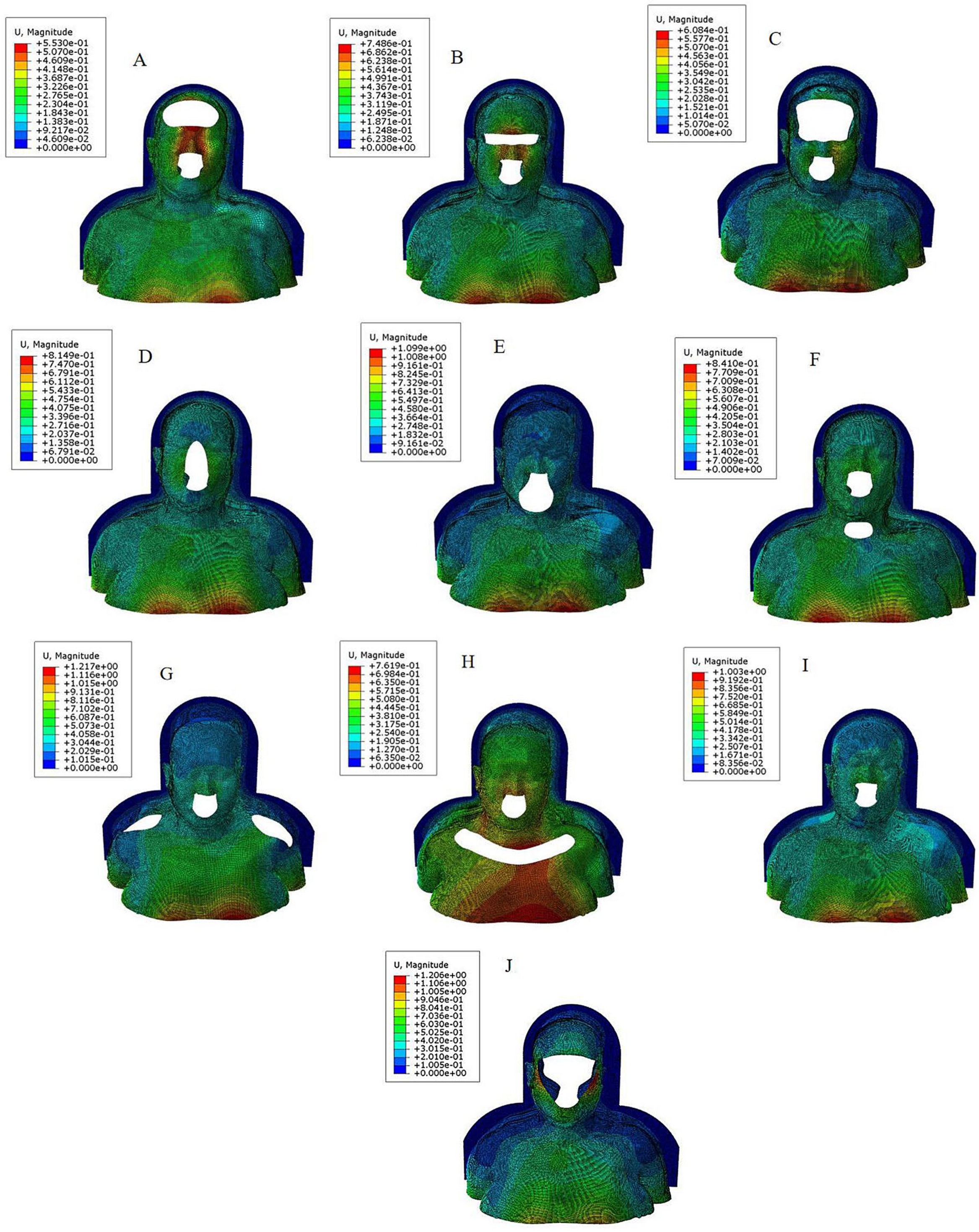

Fig. 9 The displacements of head and neck shoulder fixation molds with 10 different opening types (**A**: mouth, nostrils, and forehead; **B**: mouth, nostrils and eyes; **C**: mouth, nostrils, eyes, and forehead; **D**: mouth and nose; **E**: mouth, nostrils and chin; **F**: mouth, nostrils, and throat; **G**: mouth, nostrils, and shoulders; **H**: mouth, nostrils, and collarbone; **I**: mouth and nostrils; **J**: full face) under upward loading

near the nose, with a maximum value of approximately 0.75 cm. For model H, significant displacement near the nose is observed, around 0.59 cm. For model J, the maximum displacement is at the cheek area, with a maximum value of about 1.2 cm. Comparing these results, while model C has the largest opening area, its displacement is not as high. However, model J has the largest displacement and the poorest fixation effect. This also indicates that the position of the opening has a significant impact on the fixation effect.

In our study, we found that the impact of the mask opening area on the fixation effect differs from the common understanding. Traditionally, it is believed that larger opening areas lead to worse fixation effects, as bigger openings may cause more loosening or instability. However, our experimental results indicate that there is no direct linear relationship between the opening area and the fixation effect. Specifically, an increase in the opening area does not necessarily lead to a significant decline in the fixation effect and can even maintain stability in some cases. This finding may be closely related to the mask's structural design, the shape of the openings, and the distribution of forces. Given the anatomical variations in the head and neck regions of different patients, the structure of the mask also exhibits diversity. The irregular anatomy of the head and neck leads to an irregular 3D shape of the mask, making it impossible to simply infer the fixation effect based on the size of the opening area. For instance, larger openings may compensate for potential losses in fixation effect through optimized opening shape design. Moreover, the uniformity of force distribution may play a crucial role in maintaining fixation stability, even with larger openings. In summary, our study demonstrates that the opening area is not the sole determinant of the fixation effect. In the design process, it is necessary to consider a variety of factors, such as structure, shape, and force distribution, rather than relying solely on the conventional understanding of opening size. In future research, we will further explore other key factors that may affect the fixation effect to provide a more comprehensive theoretical basis for mask opening design.

In clinical practice, patients can experience significant involuntary body movements during treatment, which may not be limited to the two scenarios calculated in this study. Involuntary movements are influenced by psychological factors and neurological regulation, making it challenging to accurately measure the forces generated by these movements while the patient is lying on the treatment table, which can affect the accuracy of the simulations. Therefore, the force values obtained from experiments in the literature are adopted in this study. However, this force is derived from the maximum force measured on an athlete's head. Patients do not generate such a large force while lying on the treatment bed. The simulated conditions can be considered an extreme case of the model under force. As a result, the displacement values calculated in this study should be considered for semi-quantitative or qualitative analysis only. The displacement magnitude in the simulation indicates the fixation performance, while the stress magnitude reflects the comfort level to some extent. In treatment, the primary concern is the fixation effect, that is, the maximum displacement. Therefore, we focus on the impact of displacement, disregarding the impact of stress distribution.

In this study, we mainly utilized finite element software to conduct virtual simulations on the displacement conditions of mask models with different opening designs under two typical loading conditions, with a focus on the influence of different opening designs on the structural stability of the masks. In clinical practice, the positioning effect of patients is usually monitored by cone-beam CT (CBCT). In the future, we will further evaluate the fixation effect of the masks based on the CBCT images taken during the treatment of patients with mask opening requirements. This study focuses on the effect of optimizing the parameters of shape, size and position of the mask opening on the fixation effect in conventional radiotherapy. In conventional radiotherapy, patients are usually treated with cone beam CT (CBCT) for image guidance to ensure treatment accuracy.

A comprehensive analysis of Figs. 8 and 9 reveals that mask models with different structural designs exhibit differentiated displacement characteristics under mechanical loading: Under rotational and upward loading conditions, significant facial displacements are observed in models A and C, which may be associated with insufficient edge structural constraints resulting from the forehead opening design. This phenomenon suggests that local constraint reinforcement in the forehead area should be a priority, and it is recommended to enhance stability by adding reinforcement structures or optimizing the opening shape. Comparative analysis shows that the maximum displacements of models B, D, E, F, G, and I under both types of loading are concentrated in the chest edge region, which is consistent with the inherent open structural characteristics of this area in head and neck shoulder masks. The computational results validate the clinical observation that the chest edge is prone to displacement, indicating that this conventional opening design has a limited impact on overall stability. In clinical applications, the fixation effect of the chest edge area should be closely monitored. It is noteworthy that model H exhibits a significant increase in chest displacement under upward loading, confirming that clavicle area openings can significantly reduce the structural rigidity of the mask. It is recommended that when implementing clavicle area openings in clinical practice, the length of the opening should be strictly controlled, and compensatory measures such as elastic padding should be used.

The 'J' opening mask designed in this study is a proposed design for the opening that may be used in conventional radiotherapy. Displacement diagram (Figs. 8 and 9) shows that the maximum displacement of the mask under rotational load is concentrated at the edge of the chest, while under upward load, the maximum displacement is located in the cheek area, indicating that its fixation effect is direction-dependent. Notably, it is the most commonly used open design in clinical practice, has an opening shape highly similar to the 5-point commercial masks (such as the CIVCO Tranquility Series) compatible with the SGRT system. Surface Guided Radiation Therapy (SGRT) is a non-invasive and radiation-free radiotherapy positioning technique that uses an optical camera to capture 3D images of the patient's body surface in real time to monitor changes in the patient's position during the treatment process, thus ensuring the accuracy and safety of the treatment. Keane et al.'s randomized self-controlled study confirmed that, although the 5-point commercial masks have limitations in terms of inter-fraction longitudinal displacement (2.18 ± 5.76 mm) and rotational errors (e.g., roll $0.80 \pm 0.61°$) in fractionated cranial radiotherapy, dynamic error correction can be achieved through the SGRT system [23]. The results of this study further indicate that the fixation performance characteristics of the J mask are similar to those of the 5-point commercial mask, which relies on image-guided technology to compensate for inter-fraction errors. This provides important evidence for optimizing the design of open masks: while preserving patient comfort, it is necessary to specifically reinforce the mechanical support of the mask in certain loading directions (e.g., vertical load) or combine it with real-time monitoring through SGRT to improve overall positioning accuracy.

The force value used in this study differs significantly from the force value generated by patients during the treatment process. This discrepancy directly leads to differences between our calculated results and clinical reality. However, there are several reasons for selecting such a large force value. First, the force generated by patients in an unconscious state is very small. We have previously attempted calculations using a finite element model. The deformation effects produced by different models under smaller forces did not show significant differences. In this study, we aimed to observe a more pronounced deformation outcome. Choosing a larger force value for calculation can amplify the deformation effect. Additionally, from a mechanical perspective, the forces generated by humans in an unconscious state, whether in terms of the direction or absolute magnitude of force, are extremely difficult to measure. Our team collaborated with researchers specializing in mechanics to attempt related studies. We attached strain gauges and force sensors to patients' bodies to measure the forces and displacements resulting from involuntary movements. However, the quality of measurement results were poor. It is difficult to accurately assess the scope and magnitude of the force. Accurately measuring the forces generated by patients during actual treatment remains a topic for further in-depth research in the future. Therefore, we still opted to use the force values measured from athletes for our simulation calculations.

This study has several limitations. First, the effect of friction between the human body and the fixation mask was not considered in the finite element analysis. Typically, the presence of friction force would enhance the fixation effect of the mask. Second, the fixation masks currently in use are usually porous, rather than the solid material used in this experiment. Considering the convergence issues and computational costs of porous material models in finite element calculations, the study simplified the model. Therefore, this also contributes to the discrepancies between the calculated results and clinical outcomes. Lastly, this study only examined the fixation effectiveness based on opening positions. However, the opening size and shape also significantly impact fixation performance, and further quantitative studies are needed to explore these factors. We can only observe the maximum displacement and position of the surface of the head and neck mask with different opening designs and the deformation of the whole mask. Based on this information, we can take appropriate measures to enhance the fixed effect. However, this study was unable to directly quantify the specific effects of mask deformation on dose distribution, which is also a limitation of the study.

Openings in the forehead area of thermoplastic masks have the most pronounced impact on fixation effectiveness in the facial region. This finding suggests that in clinical practice, the design of openings in the forehead area should be approached with caution. The purpose of this study was to analyze the effect of opening position and area of thermoplastic film on the fixation effect according to the actual situation of patients. It is expected to provide patients with a comfortable and effective fixation method and improve the accuracy and effectiveness of treatment.

Conclusion

This study employed finite element analysis to investigate the impact of opening configurations in thermoplastic fixation masks on fixation effectiveness in radiation therapy. The location of the opening significantly affects the fixation performance of the thermoplastic masks. In particular, openings in the forehead area of thermoplastic masks have the most pronounced impact on fixation effectiveness in the facial region. This finding suggests that in clinical practice, the design of openings in the forehead area should be approached with caution. This research offers insights into the fixation effectiveness and comfort of thermoplastic masks and provides valuable references for future personalized medical applications.

Author contributions

Y L conceived and designed the study; Y N. X acquired the data; G B. P and Y Q. M performed the computational modeling and drafted the manuscript; J B.

S supported this study and shared ideas of the analysis. All authors read and approved the final manuscript.

Funding
This work was supported by the Central Leading Science and Technology Development Foundation of Shanxi Province (Number: YDZJSX20231A064) and the Science Fundation of Shanxi Bethune Hospital (2023YJ08).

Data availability
No datasets were generated or analysed during the current study.

Declarations

Ethics approval and consent to participate
This study was approved by the Ethics Committee of Shanxi Bethune Hospital (YXLL-2022-127), and strictly complied with the relevant regulations of medical ethics and the requirements of patients' informed consent.

Consent for publication
All the authors approved the consent for publication.

Competing interests
The authors declare no competing interests.

Received: 27 September 2024 / Accepted: 24 April 2025
Published online: 29 April 2025

References

1. Thompson-Harvey A, Yetukuri M, Hansen AR, et al. Rising incidence of late-stage head and neck cancer in the united States. Cancer. 2020;126(5):1090–101.
2. Mody MD, Rocco JW, Yom SS, et al. Head and neck cancer. Lancet. 2021;398(10318):2289–99.
3. Siegel RL, Miller KD, Jemal A. Cancer statistics, 2018. Cancer J Clin. 2018;68(1):7–30.
4. Guo K, Xiao W, Chen X, et al. Epidemiological trends of head and neck cancer: A population-based study. Biomed Res Int. 2021;2021(10):1–14.
5. Amini A. An updated review on head and neck cancer treatment with radiation therapy. Cancers. 2021;13(19):4912–4912.
6. Li G, Jiang Y, Li G, et al. Comprehensive analysis of radiosensitivity in head and neck squamous cell carcinoma. Radiother Oncol. 2021;159(0):126–35.
7. Hutchinson MK, Mierzwa M, Dsilva N. Radiation resistance in head and neck squamous cell carcinoma: dire need for an appropriate sensitizer. Oncogene. 2020;39(18):3638–49.
8. Budrukkar A, Guinot JL, Tagliaferri L, et al. Function preservation in head and neck cancers. Clin Oncol. 2023;35(8):497–506.
9. Brook I. Late side effects of radiation treatment for head and neck cancer. Radiat Oncol J. 2020;38(2):84–92.
10. Sgouros G, Bodei L, Mcdevitt MR, et al. Radiopharmaceutical therapy in cancer: clinical advances and challenges. Nat Rev Drug Discovery. 2020;19(9):589–608.
11. Park S, Kim E, Choi N, et al. A phase II trial of neoadjuvant nivolumab, docetaxel, and cisplatin therapy followed by surgery and radiation therapy for resectable high-grade salivary gland carcinoma. J Clin Oncol. 2023;41(16suppl):TPS6110–6110.
12. Mercke C, Wickart-Johansson G, Sjödin H, et al. Radiotherapy—Dose escalated for large volume primary tumors—And cetuximab with or without induction chemotherapy for Hpv associated squamous cell carcinoma of the head and neck—A randomized phase II trial. Cancers. 2023;15(9):2543–2543.
13. Ahmed LA, Darwish HAA, El-Haddad S, et al. Effect of protracted radiotherapy treatment on outcome of head and neck SCC patients (NEMROCK experience). Ann Oncol. 2016;27(0):vi347–347.
14. Peng X, Li Z, Pei Y et al. Streptococcus salivarius K12 alleviates oral mucositis in patients undergoing radiotherapy for malignant head and neck tumors: A randomized controlled trial. Journal of Clinical Oncology. 2024;0 (0).
15. Qi XS, Hu AY, Lee SP, et al. Assessment of interfraction patient setup for head-and-neck cancer intensity modulated radiation therapy using multiple computed tomography-based image guidance. Int J Radiat Oncol Biol Phys. 2013;86(3):432–9.
16. Djordjevic M, Sjöholm E, Tullgren O, et al. Assessment of residual setup errors for anatomical sub-structures in image-guided head-and-neck cancer radiotherapy. Acta Oncol. 2014;53(5):646–53.
17. Hirotaki K, Tomizawa K, Moriya S, et al. Impact of anatomical position errors on dose distribution in head and neck radiotherapy and robust image registration against anatomical changes. Anticancer Res. 2023;43(4):1827–34.
18. Fukao M, Okamura K, Sabu S, et al. Repositioning accuracy of a novel thermoplastic mask for head and neck cancer radiotherapy. Phys Med. 2020;74:92–9.
19. Contesini M, Guberti M, Saccani R, et al. Setup errors in patients with head-neck cancer (HNC), treated using the intensity modulated radiation therapy (IMRT) technique: how it influences the customised immobilisation systems, patient's pain and anxiety. Radiat Oncol. 2017;12(1):72.
20. Nixon JL, Cartmill B, Turner J, et al. Exploring the prevalence and experience of mask anxiety for the person with head and neck cancer undergoing radiotherapy. J Med Radiat Sci. 2018;65(4):282–90.
21. Elsner K, Naehrig D, Halkett GKB, et al. Reduced patient anxiety as a result of radiation therapist-led psychosocial support: A systematic review. J Med Radiat Sci. 2017;64:220–31. [CrossRef] [PubMed].
22. Lastrucci A, Morelli I, Votta C, et al. Open-Face masks in radiotherapy: enhancing therapeutic strategies for head and neck and brain Cancer Patients—A. Compr Scoping Rev Cancers. 2024;16(16):2899–2899.
23. Michèle Keane N, Weitkamp I, Madani, et al. Randomized self-controlled study comparing open-face vs. closed immobilization masks in fractionated cranial radiotherapy. Radiother Oncol. 2024;0(0):110314–110314.
24. Chen X, Lu L, Wang Y, et al. Surface guided radiation therapy with an innovative open-face mask and mouth bite: patient motion management in brain stereotactic radiotherapy. Clin Translational Oncol. 2023;26(2):424–33.
25. Fisher M, Applegate C, Ryalat MH, et al. Evaluation of 3-D printed immobilisation shells for head and neck IMRT. Open J Radiol. 2014;04(04):322–8.
26. Chen S, Lu Y, Hopfgartner C et al. 3-D Printing based production of head and neck mask for radiation therapy using CT volume data: a fully automatic framework. 2016 IEEE 13th International Symposium on Biomedical Imaging (ISBI).
27. Loja MAR, Craveiro DS, Vieira L et al. Radiotherapy-customized head immobilization masks: from modeling and analysis to 3D printing. Nuclear Science and Techniques. 2019;30 (9).
28. Almosnino S, Pelland L, Stevenson JM. Retest reliability of force-time variables of neck muscles under isometric conditions. J Athl Train. 2010;45(5):453.
29. Chen J, Teng YC, Shu D, et al. Automated robotic-assisted patient positioning method and dosimetric impact analysis for Boron neutron capture therapy. Sci Rep. 2024;14(1):28995.

Publisher's note